11B.4 Assessment of calibration performance of the geostationary satellite imager visible channel in the ISCCP B1 data

Anand K. Inamdar[1] & Kenneth Knapp

1. Introduction

The International Satellite Cloud Climatology Project (ISCCP) was established in 1982 as part of the World Climate Research Program (WCRP), with the objective of collecting and analyzing the satellite radiance values from both the Polar Orbiting Environmental Satellites (POES) and geo-stationary meteorological (GEO) satellites to infer the global cloud climatology and its impact on the earth's radiation budget. Data collection began in 1983 (Schiffer and Rossow, 1983) through setting up of Sector Processing Centers (SPC) worldwide which received the full-resolution raw GEO data from GOES (East and West), GMS, INSAT and METEOSAT as well as data from NOAA polar obiters. These were sub-sampled to 10 km and 3 hourly resolution (creating so-called B1 data) and set aside for archiving due to computing, storage and processing limitations at the time. The ISCCP Global Processing Center (GPC) was instead provided with further sub-sampled reduced resolution (30 km and 3 hourly) data (B2), leaving the B1 data languishing in the archive until 2003. NOAA/NCDC (Knapp, 2008a) initiated the rescue efforts for the B1 data by developing documentation, read software, data quality testing and calibration. Full details of scientific data stewardship operations, description and evolution of the B1 data are provided by Knapp (2008a).

ISCCP B1 data will be employed in the reprocessing of the cloud products resulting in a higher resolution ISCCP cloud climatology, improved cloud detection (Rossow and Gardner, 1993), cloud optical depth, precipitation, surface albedo (Govaerts et al 2008), and surface radiation budget (SRB), etc. Among other applications, the B1 data has been successfully employed in hurricane research and precipitation monitoring in data-sparse regions (Knapp et al 2011; Kossin et al, 2006; Knapp and Kossin, 2007). The primary common channels among the earlier GEOs were the visible (0.67 μm) and the

[1]*Corresponding author address*: Anand K. Inamdar, CICSNC/NOAA/NCDC, 151 Patton Avenue, Asheville NC 28801, e-mail: anand.inamdar@noaa.gov

Infrared (IR) Window (11 μm). The IR water vapor channel at 6.7 μm became available on later satellites. The IR channels have already been calibrated (Knapp, 2008b). The visible channels have been calibrated by normalizing with the concurrent Advanced Very High Resolution Radiometer (AVHRR) on the afternoon NOAA polar-orbiting weather satellite at the same viewing geometry (Desormeaux et al 1993). However, since ISCCP began in 1983, there was no calibration prior to that. Also independent assessments (Knapp, 2008a) have revealed certain inconsistencies. The present study discovered discrepancies particularly in the ISCCP calibration of Meteosat, GMS and MTSAT series. Recently an improved and Moderate Resolution Imaging Spectroradiometer (MODIS) – compatible AVHRR visible channel calibrated Climate Data Record (CDR) product (Heidinger et al 2010) has become available. The present study reports results of cross-calibration with the CDR product and comparison with the ISCCP calibration.

2. Match-up Data

The reference data used in this study is the solar reflectance calibration in the AVHRR Pathfinder Atmospheres Extended (PATMOS-x) dataset (Heidinger et al 2010). These represent a set of calibration coefficients for all of the AVHRR sensors (including those in the morning orbits) derived from a consistent approach traceable to the MODIS standard. Channel 1 (0.63 mm) reflectance values have been derived employing 4 different sources including 1) Simultaneous Nadir Overpass (SNO) with MODIS for the MODIS era (years 2000+), 2) an Antarctic target, 3) Libyan desert target, and 4) AVHRR to AVHRR SNO's. The Antarctic and Desert targets have been assumed to be radiometrically stable over time and have been used as reference during the pre-MODIS era after they have been characterized by MODIS. Thus the methodology employed in the calibration of the solar reflectance channel in the PATMOS-x data is radiometrically tied to the MODIS imager and guarantees continuity in satellite-to-satellite transitions.

3. Methodology

3.1 Definitions

The integrated radiance, $\boldsymbol{L}$ (W m^{-2}), over the visible spectral channel is expressed in terms of the detector-measured raw counts, $\boldsymbol{X}$, and instrumental spectral response function, $S(\lambda)$, as,

$$L=\int_0^\infty L_\lambda S(\lambda)d\lambda=a_0+a_1X \qquad (1)$$

where a_0 is the intercept and a_1 is the calibration slope. The scaled radiance is $\pi L/F_0$, where F_0 is the incident solar flux at the top of the atmosphere weighted by the instrumental spectral response. Thus,

$$F_0=\int_0^\infty E_0(\lambda)S(\lambda)d\lambda,$$

with $E_0(\lambda)$ being the extra-terrestrial solar flux at wavelength, λ. The instrument-independent bi-directional or isotropic reflectance, ***R***, is derived from the scaled radiance by normalizing with the cosine of the incident solar zenith angle, μ_0, and correcting for the mean earth-sun distance, ***d***, as

$$R=\frac{\pi L}{F_0(\mu_0 / d^2)} \qquad (2)$$

3.2 Cumulative Histogram Matching Technique

Calibration can be performed by matching up concurrent (spatial and temporal) imagery from the GEO and AVHRR. The matching criteria used here are: 1) observations are within 10 minutes (ensures similar solar zenith angles); 2) solar zenith angle less than 59 degrees; 3) difference in cosine of satellite view angles less than 0.05, and 4) for off-nadir view angles, difference in azimuth angles less than 15 degrees. For nadir views emitted radiation is assumed isotropic and so no azimuth restriction is imposed.

A major problem in calibration is the spatial and temporal matching of data from the two sensors on an exact pixel-to-pixel level. It is a fact that even at nominal wind speeds, clouds can move one pixel per minute making it difficult for the sensors spaced as much as 10 minutes apart to be viewing the same imagery for a pixel. Yet it is assumed that the general features of the imagery remain identical, implying the distribution of brightness are similar even when images are spaced 10 minutes apart. For this reason, we follow a histogram matching technique here instead of a simple linear regression. Histogram matching has been successfully employed in sensor calibration studies (Kidder et al, 2006), land use change detection, etc. (Richards and Jia, 1993).

The bi-directional reflectance, ***R***, (Eq 2) for both the matched images (GEO and AVHRR) should be similar. So the absolute radiance, ***L*** (W m^{-2}) for GEO visible sensor can be obtained from Eq (2) by employing F_0, as the extra-terrestrial incident solar flux integrated over the GEO visible spectral channel.

Histogram matching is widely used in digital image processing. Here the histogram of a given image is matched to the histogram of a reference image. The concept is illustrated through matching of GOES-8 and AVHRR imagery for Feb 2001 in Fig. 1 (see embedded text in the caption for explanation). Note that the calibration derived from the histogram matching scheme is in very close agreement with the ISCCP calibration.

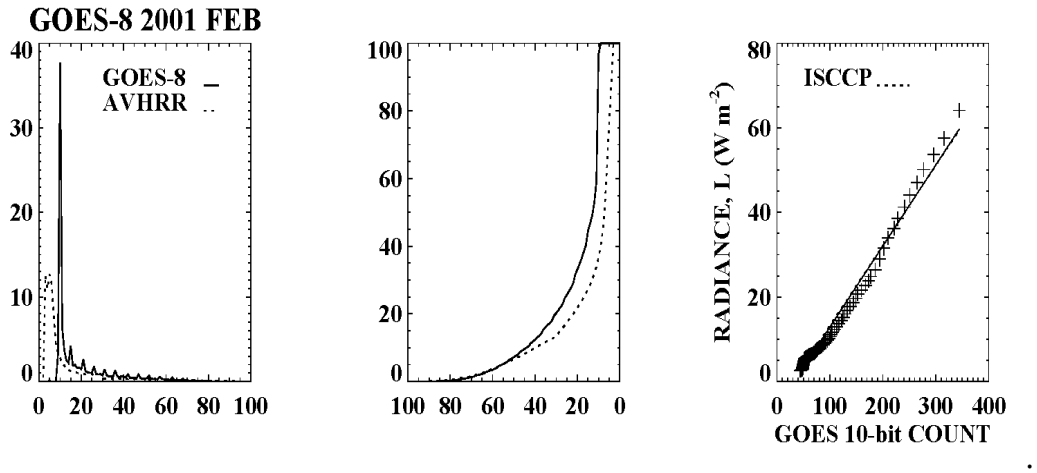

Fig. 1. Left: Histogram of the distribution of GOES raw counts (10-bit count normalized to 0 - 100) and radiance (L, W m^{-2}) derived from the match-up (also normalized to 0-100); middle: Inverse cumulative histogram derived from the distribution on the left panel; right: Matched-up pairs (represented by symbols) of GOES counts and Radiance for equal cumulative probability shown in the middle panel. The solid line is the least squares fit through the symbols and the dashed line (almost merged with the solid line here) represents the ISCCP calibration.

4. Results and Discussion

GEO and AVHRR data are matched for each month as described in the previous section to obtain the calibration slope, a_1, (Eq. 1). A steady value for the slope indicates a stable sensor calibration. But generally sensors degrade over time and time variation of a_1 can be expressed (assuming a linear variation with time) as,

$$a_1 = g_0 + g_1(DSL) \qquad (3)$$

where *DSL* is the number of days or a measure of time lapsed after launch.

The calibration slopes have been derived for each of the GEO satellites for each month for the life of the sensor employing the histogram matching scheme described in the previous section. The slope of the time series of the calibration slopes is a measure of the degradation of the visible sensor during its lifetime, and are shown for selected GEOs in Figs. 2 – 4. The slopes derived from the present approach follow the ISCCP calibration closely for GOES (Fig. 2). Notice that for GOES-7, although the two calibration curves track the inter-annual variation very nicely from 1987-1992, the ISCCP calibration is characterized by lot of noise during the post-Pinatubo eruption (after 1992) period.. There are gaps during 1998 (GOES-8) when no match-ups were available for solar zenith angles below 60 degrees. The GOES-8 sensor shows faster degradation than GOES-5, 6 or 7. The ISCCP calibration slope is slightly systematically lower (Fig. 3) for the Meteosat series. The time series of calibration slopes for the GMS series again demonstrate the close agreement with the ISCCP. The calibration slope derived from both ISCCP and the present approach display a dip during 1998-2001 period for

GMS-5 (Fig. 4). The ISCCP calibration for MTS-1 (which replaced the GMS series) not only displays more noise, but is characterized by a large systematic offset, which needs further investigation.

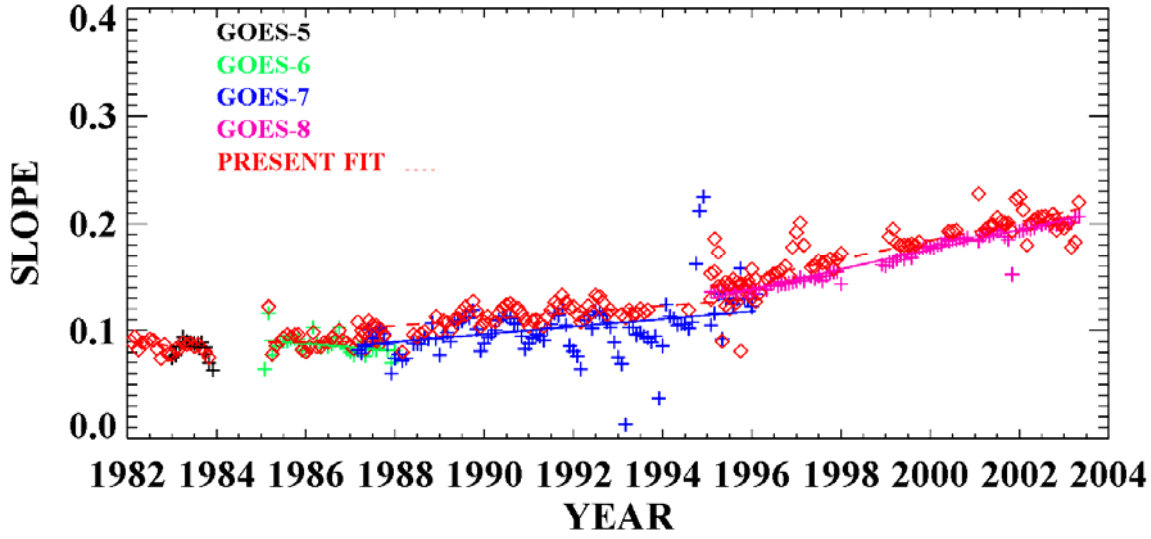

Fig. 2. Time series of calibration slope for GOES-5 to GOES-8 (1982 – 2004). The '+' symbols and the solid lines refer to the ISCCP and the diamond symbols and the associated regression fit line (dashed) are from the present calibration approach.

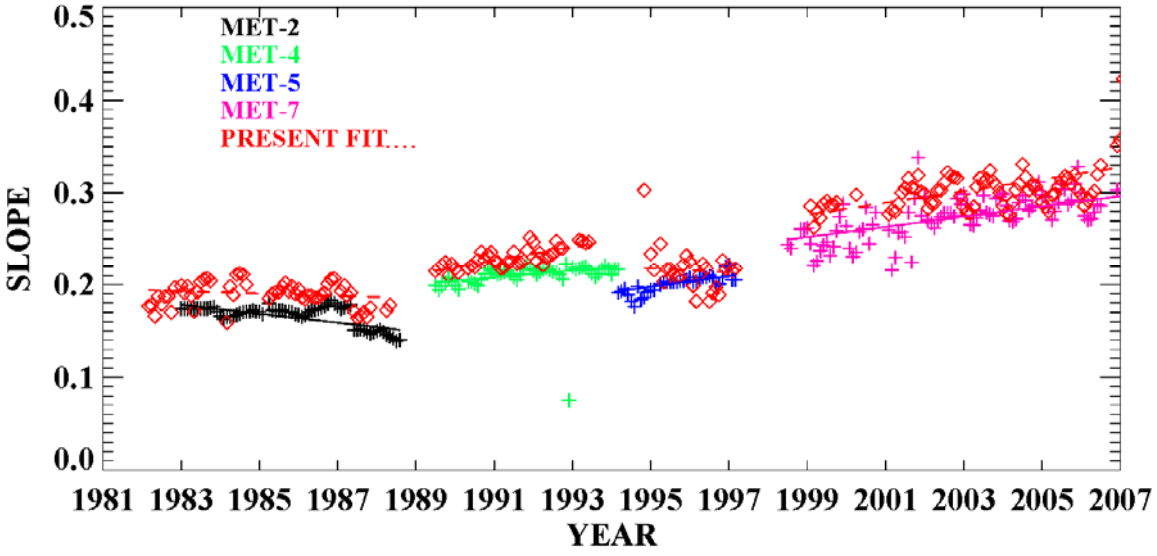

Fig. 3. Same as Fig. 2, but for the Meteosat series (MET-2, MET-4, MET-5 and MET-7).

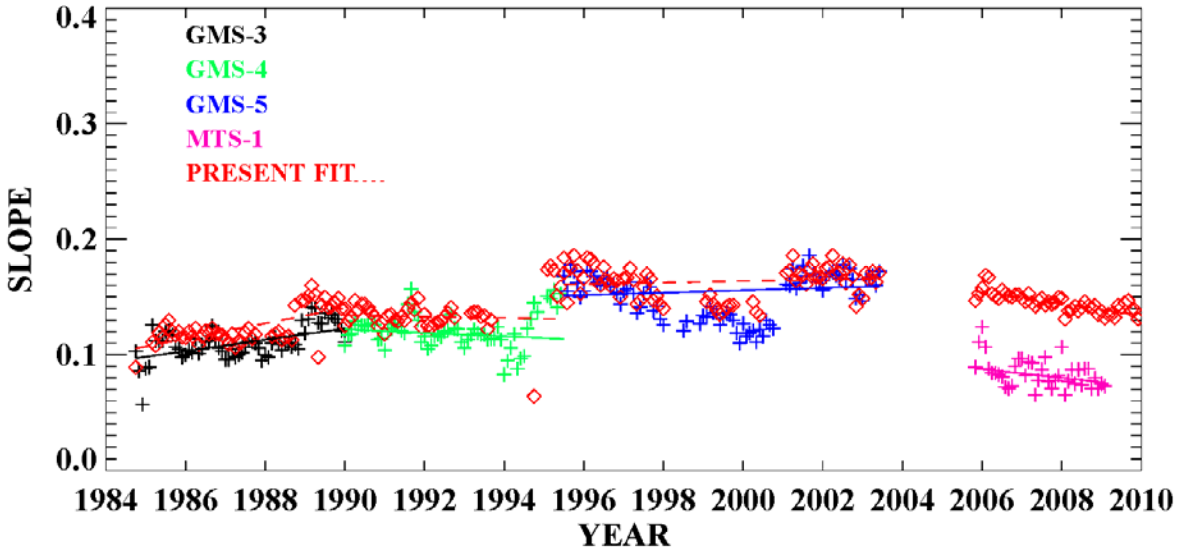

Fig. 4. Same as Fig. 3, but for the GMS series GMS-3, GMS-4, GMS-5 and MTSAT (MTS-1) satellite.

5. Summary and Conclusions

The recent rescue of the ISCCP-B1 data (Knapp 2008a, Knapp et al 2011) has provided climate researchers with a data set rich in climate information for the period 1978 through the present. This dataset will be incorporated in a future reprocessing of the ISCCP cloud climatology resulting in a higher spatial resolution of the cloud properties and surface radiation budget. The infrared channels have been already calibrated and the present study takes advantage of a recent CDR with well-calibrated AVHRR visible channel to verify and fill in gaps in the existing GEO visible calibration. Calibration of some of the pre-1983 GOES visible channel has been hampered due to non-availability of the spectral response functions, and efforts are continuing through contacting different sources. While the time series of ISCCP calibration slopes tracks results obtained from the present calibration approach for the most part, a few cases of systematic differences have been identified (especially MET and MTS-1 satellites).

References

Govaerts, Y. M., A. Lattanzio, M. Taberner and B. Pinty, 2008: Generating global surface albedo products from multiple geostationary satellites, *Remote Sensing of Environment*, doi:10.1016/j.rse.2008.01.012

Heidinger, A. K., W. C. Straka III, C. C. Molling, J. T. Sullivan, and X. Wu, 2010: Deriving an inter-consistent calibration for the AVHRR solar reflectance data record. *Int. J. Remote Sensing*, 31, 6493-6517.

Kidder, S. Q., and A. S. Jones, 2006: A blended satellite total precipitable water product for operational forecasting. *J. Atmos. Ocean. Technology*, 24, 74-81.

Knapp, K. R. and J. P. Kossin, 2007: New global tropical cyclone data from ISCCP B1 geostationary satellite observations. *Journal of Applied Remote Sensing*, **1**, 013505.

Knapp, K. R., 2002: Quantification of aerosol signal in GOES-8 visible imagery over the U. S. *J. Geophys. Res.*, 107, (doi: 10.1029/2001JD002001).

Knapp, K. R., 2008a: Scientific stewardship of International Satellite Cloud Climatology Project B1 global geostationary observations. *J. Applied Remote Sensing*, 2, 2-19.

Knapp, K. R., 2008b: Calibration of long-term geostationary infrared observations using HIRS. *J. Atmos. and Oceanic Technology*, **5** (2), 183-195, doi:10.1175/2007JTECHA910.1.

Knapp, K. R. and co-authors, 2011: Globally gridded satellite observations for climate studies. *Bull. Amer. Metoer. Soc*., 92, 893-907, doi: http://dx.doi.org/10.1175/2011BAMS3039.1

Richards, J.A., and X. Jia, 1993: Remote Sensing Digital Image Analysis - An Introduction. Springer - Verlag, Berlin, 469 pp

Rossow, W. B., and L. C. Gardner, 1993: Cloud detection using satellite measurements of infrared and visible radiances for ISCCP. *J. Clim*., 6, 2341-2369.

Rossow, W. B., and R. A. Schiffer, 1991: ISCCP Cloud Data Products. *Bull. Am. Meteor. Soc.*, 72, 2-20.